ISSN: 2349-5162 | ESTD Year: 2014 | Monthly Issue



JOURNAL OF EMERGING TECHNOLOGIES AND INNOVATIVE RESEARCH (JETIR)

An International Scholarly Open Access, Peer-reviewed, Refereed Journal

Study the Radiation Shielding Properties of Metal Hydride used in Hydrogen Storage

¹Pradip Devkota, ²Madhu Pandev

¹Department of Physics, Amrit Science Campus, Lainchaur, Kathandu, Nepal

Abstract: This article investigates the influence of coherence scattering on the Total Attenuation Coefficient (TAC) of various metal hydrides within the energy spectrum. The primary objective is to discern the impact of coherence scattering on attenuation behavior and identify distinctive trends in different energy regions. The methodology involves utilizing the XCOM software to generate TAC profiles for metal hydrides both with and without coherence scattering. Findings indicate that TAC with coherence scattering aligns closely with the non-coherence counterpart in the higher energy region, signifying diminished influence. However, in the lower energy range (below 1 MeV), a significant divergence is observed, highlighting the substantial role of coherence scattering in altering attenuation characteristics. Notably, FeTiH2 and Mg2NiH2 exhibit two distinct deep points and peak points, setting them apart from other metal hydrides. The study recommends careful consideration of coherence scattering effects in applications requiring precise control over radiation attenuation. These insights are crucial for material design and optimization, offering avenues for tailored attenuation properties in diverse energy scenarios. The nuanced understanding of coherence scattering's impact contributes to advancements in fields such as materials science, radiation shielding, and hydrogen storage, where detailed knowledge of attenuation behavior is paramount.

IndexTerms - Total Attenuation Coefficient, metal hydrides, coherence scattering, non-coherence XCOM software, radiation shielding, and hydrogen storage

1. Introduction

Metal hydrides are compounds formed by the reaction of metals with hydrogen. They are known for their ability to reversibly absorb and release hydrogen gas, making them valuable materials for hydrogen storage applications. Each of the mentioned metal hydrides has unique properties that contribute to their effectiveness in storing hydrogen: NaAlH4 (Sodium Alanate), A complex metal hydride known for its high hydrogen storage capacity. MgH₂ (Magnesium Hydride), Widely studied for its high hydrogen storage capacity, but challenges include slow kinetics. LiAlH₄ (Lithium Alanate), Exhibits high hydrogen storage capacity, but its use is limited by high operating temperatures. Mg₂NiH₄ (Magnesium Nickel Hydride), Known for improved kinetics compared to pure magnesium hydride. CaH2 (Calcium Hydride), Offers high hydrogen storage capacity but faces challenges related to reversibility. LiBH₄ (Lithium Borohydride), Attracts attention for its high hydrogen density, but challenges include high desorption temperatures. FeTiH₂ (Iron Titanium Hydride), Known for its potential as a hydrogen storage material due to a combination of iron and titanium. While these metal hydrides show promise for hydrogen storage, the literature lacks comprehensive studies on the effects of high-energy radiation on their performance. This research gap underscores the need for investigations into the impact of radiation on the properties and safety of these metal hydrides, providing valuable insights for the advancement of hydrogen storage technology.

1.2 Mass attenuation coefficient

The mass attenuation coefficient, often denoted by the symbol $\frac{\mu}{\rho}$, is a fundamental parameter in the field of radiation physics and material science. It quantifies how a material attenuates or reduces the intensity of a beam of radiation as it passes through. The mass attenuation coefficient is expressed in units of cm²/g and represents the probability of interaction between the incident radiation and the atoms of the material per unit mass. The mass attenuation coefficient is a critical parameter in understanding how radiation interacts with matter. This coefficient can be categorized into with coherence $\left(\frac{\mu}{\rho}\right)_w$ and without coherence $\left(\frac{\mu}{\rho}\right)_{nw}$, depending on whether the phase information of the scattered radiation is considered. In situations involving coherent scattering,

where incident photons interact with the entire atom, the phase relationship is preserved, and this is termed with coherence. On the other hand, incoherent scattering processes, such as Compton scattering, involve interactions with individual electrons, resulting in a loss of phase relationship and are referred to as without coherence. The total mass attenuation coefficient for a material is a combination of these components, providing a comprehensive understanding of how radiation is attenuated as it passes through different substances. This distinction is crucial for accurate modeling and interpretation of radiation-matter interactions in various contexts, contributing to advancements in fields such as medical imaging, industrial processes, and materials science.

²Department of Physics, Patan Multiple Campus, Patandhoka, Lalitpur, Nepal

1.3 Research gap and motivation

The existing challenge in hydrogen storage systems, stemming from the limitations of gaseous and liquid forms in terms of volume, safety, and transportability, has spurred significant interest in solid-state hydrogen storage. This emerging research field seeks to overcome these drawbacks by utilizing solid materials, offering advantages such as high energy density, enhanced safety without the need for extreme pressures or cryogenic conditions, stable hydrogen absorption/release cycles, and ease of transport. Notably, metal hydrides, chemical hydrides, and carbon-based materials have shown promise in providing efficient and reversible hydrogen storage in solid form. However, a research gap is evident, as the literature lacks investigations into the effects of highenergy radiation on various metal hydrides used for solid-state hydrogen storage. This gap serves as a motivation for future research, emphasizing the need to explore the impact of high-energy radiation on the performance and safety of different metal hydrides, thereby contributing valuable insights to the advancement of hydrogen storage technology.

2. Literature review

2.1 NaAlH₄ (Sodium Alanate)

Sodium alanates, particularly NaAlH₄, present an economical and high-capacity solution for reversible hydrogen storage, with investigations into NaAlH₄ and NaAlH₄ in this context. Utilizing mechanical grinding and chemical modification enhances reaction kinetics, and at 150–180°C, the hydrides demonstrate a significant reversible capacity of approximately 4.5–5 wt% [1]. Despite NaAlH₄ being considered for hydrogen storage, challenges in regeneration persist. Catalysts like HfCl₄, VCl₃, TiO₂, TiCl₃, and Ti influence the decomposition temperature, with TiO₂ exhibiting the most positive effect, while co-dopants such as activated carbon and graphite improve hydrogen diffusion in desorbed/reabsorbed samples [2]. Although sodium alanate's intricate structure garners attention for hydrogen storage, a separate study reveals the addition of Ti, C, and H atoms acting as catalysts, influencing stability [3]. Notably, the higher band gap values in pure Na1₂Al1₂H₄₈ clusters suggest increased stability, underscoring sodium alanates' potential for effective hydrogen storage. However, it's crucial to highlight that radiation effects on these materials have not been explored to date on this materials.

2.2 MgH₂ (Magnesium Hydride)

Efficient energy storage is pivotal for widespread utilization of renewable energy, posing a significant challenge. Magnesium hydride (MgH₂) emerges as a promising energy carrier, boasting advantages such as low cost, abundant supply, and high energy storage capacity [4]. Strategies to enhance MgH₂'s hydrogen storage performance include catalyst doping, MgH₂ nanosizing, alloying, and composite system construction. Notably, catalyst doping and MgH₂ nanosizing prove to be particularly effective modifications [5]. The mass storage of hydrogen presents challenges for large-scale industrial applications and continuous distribution, especially for future environmentally friendly energy carriers. Nevertheless, Hydrogen Solid State Storage (HSSS) using MgH₂ bodies has demonstrated feasibility in terms of process and safety. Early experiments at McPhy Energy showcased the production of reactive MgH₂-based pellets at a capacity of approximately 27 tons/year, utilizing unique and self-built installations [6].

2.3 LiAlH₄ (Lithium Alanate)

Lithium aluminum hydride (LiAlH₄), boasting a high hydrogen capacity of 10.5 wt%, stands out as a promising solid-state hydrogen storage material for onboard hydrogen fuel cell systems. Despite its potential, practical application faces challenges due to insufficient dehydrogenation kinetics and cycling behaviors. Addressing these limitations, research suggests that Al₂Ti can enhance the adsorption and splitting of H₂, contributing to the rehydrogenation of LiAlH₄ [7]. While LiAlH₄ is considered a viable material for solid-state hydrogen storage, its lack of reversibility and slow kinetics hinder practical use. Nevertheless, under specific conditions, desorbed LiAlH₄ can be partially regenerated at 8 MPa H₂ and 150 °C. Investigations into the pressurecomposition isotherm indicate altered equilibrium states within nanoscale voids, suggesting potential adjustments to hydrogen thermodynamic paths [8].

2.4 Mg₂NiH₄ (Magnesium Nickel Hydride)

Through an examination of growth kinetics, crystal structure, and chemical bond energies, it is established that the interface between MgNi2 and Mg2NiH4 serves as the likely site for the growth reaction. Mg2NiH4 is identified as an indirect gap semiconductor with a gap value of ~1.6 eV, yet luminescence beyond the band gap is observed [9]. The direct formation of Mg₂NiH₄ occurs by exposing a pressed mixture of MgH₂ and Ni powders to a hydrogen atmosphere at 450 °C, demonstrating pressure invariability during synthesis. XRD and TDS methods determine the quantity of Mg₂NiH₄, while SEM with EDX microanalysis examines reaction product morphology. Exploring the impact of exposure time and synthesis temperature reveals insights into the reaction yield [10]. Addressing challenges in magnesium-based hydrogen storage, a carbon-covered nanocrystalline Mg₂NiH₄ sample exhibits reduced dehydrogenation enthalpy (from $89.9 \pm 4.0 \text{ kJ/mol}$ to $67.0 \pm 0.5 \text{ kJ/mol}$) and maintained cycling kinetics after ten cycles. The enhanced hydrogen storage property results from a synergistic effect involving alloying, carbon covering, and nanocrystalline strategies [11].

2.5.CaH₂ (Calcium Hydride)

Research explored the use of calcium hydride and lithium hydride for hydrogen storage in alkaline fuel cells, demonstrating their suitability for a 1 kW unit using water vapor. The hydrogen production reaction exhibits first-order dependence on water vapor pressure [12]. An on-site hydrogen generator using calcium hydride (CaH₂) mixed with resin enables controlled hydrogen production at a moderate rate when reacting with water [13]. Calcium hydride's potential as a hydrogen and energy storage material is investigated, addressing challenges like high operating temperature. The study provides essential thermodynamic properties for molten and solid CaH₂ after a gap of over 60 years [14].

2.6 LiBH₄ (Lithium Borohydride)

The Density Functional Theory (DFT) with the Perdew-Burke-Ernzerhor for solids (PBEsol) approach was employed to apply single, double, and triaxial strains to lithium borohydride (LiBH₄). The results reveal structural changes with deformation amplitude, classifying LiBH₄ as an insulator with a band gap of 6.73 eV. Triaxial deformation requires more energy than single and double strains, contributing to decreased thermodynamic properties. Compressive strains of $\varepsilon = -9\%$ lead to a 3.25% decrease in enthalpy of formation and a 36.54% drop in decomposition temperature. Tensile strains of $\varepsilon = +9\%$ result in a 3.85% decrease in enthalpy of formation and a 26.44% drop in decomposition temperature. These findings align with U.S. Department of Energy

standards for solid-state hydrogen storage [15]. Additionally, research highlights challenges in achieving high-density hydrogen storage and explores the catalyzed hydrogen desorption from LiBH4, showcasing potential applications [16].

2.7 FeTiH₂ (Iron Titanium Hydride)

TiFe alloys exhibit high hydrogen storage density, making them valuable for room temperature hydrogen absorption/desorption. While promising for various applications, challenges include activation difficulties and toxicity concerns. The review covers current research, performance, phase structures, and applications, offering insights and future directions [17]. Efficient hydrogen storage is essential for clean energy, and surface adsorption on nanoporous materials, explored through electrospun nanofibers and MOFs, emerges as a promising solution. The study addresses hydrogen storage challenges, emphasizing viable storage methods. Hydrogen storage is crucial for its use in car transportation. This tutorial review outlines existing technologies, focusing on hydrogen cars, and explores advancements like plasma hydrogen ion implantation. It serves as a guide for researchers and enthusiasts, providing insights into hydrogen storage for innovative applications [18].

The examined literature extensively discusses various hydrogen storage materials, including sodium alanates, lithium borohydride, magnesium hydride, calcium hydride, and TiFe alloys. However, none of the sources explicitly addresses the study of radiation effects on these metal hydrides used in hydrogen storage. The impact of radiation on the properties and performance of these materials for hydrogen storage is not explored in the provided information.

3. Materials and methods

3.1 XCOM software

The NIST XCOM software, developed by the National Institute of Standards and Technology, serves as a critical tool for researchers in radiation physics and materials science. With a user-friendly online interface, it offers essential photon cross-section data for elements, compounds, and mixtures, facilitating studies in radiation shielding design and computational research. Users can access the database online or download a copy for offline use. XCOM provides two modes of usage, including a text-based version and a feature-rich version with advanced capabilities. Widely recognized as one of the oldest web-based programs for photon cross-section calculations, XCOM continues to play a crucial role in research, education, and computational studies related to photon interactions with matter. The XCOM photon attenuation database tool allows the user to choose the chemical composition (element, compound and mixture) of interest and provides a wide range of gamma photon attenuation data in the energy range of 1 keV and 100 GeV. The tool provides the mass attenuation coefficient values, comprising photon matter interaction phenomena such as photoelectric absorption, scattering (incoherent and coherent) and pair production (nuclear and electronic fields). However, the number of data points obtained from one composite to another are different.

3.2 Lambert-Beer law

The Lambert-Beer Law, also known as Beer's Law or the Beer-Lambert Law, is a fundamental principle in the field of spectroscopy. It describes the relationship between the concentration of a solute in a solution and the absorbance of light as it passes through the solution. The absorption coefficient μ can be derived from the Lambert-Beer law

$$I = I_0 e^{-\mu t} \tag{1}$$

Where I_0 is the incident intensity when measured without sample, I is intensity transmitted through the sample, and t is the sample thickness (cm). The absorption coefficient (μ) is calcauted by using [19].

$$\mu = \frac{1}{t} \ln \left(\frac{I_0}{I} \right) \tag{2}$$

However, if the XCOM software includes features related to the attenuation of photons as they pass through materials, the Lambert-Beer Law could be indirectly applicable. In this case, the principles of absorption and attenuation could be analogous to the Lambert-Beer Law, where the attenuation of photons is related to the material's characteristics, such as its composition and thickness.

3.3 Total attenuation coefficient radiation shielding

The total attenuation coefficient in radiation shielding, often denoted as μ , represents the combined effect of various processes that attenuate radiation as it passes through a material. These processes include photoelectric absorption, Compton scattering, and pair production. The XCOM software, developed by the National Institute of Standards and Technology (NIST), is a powerful tool for calculating photon cross-section data, including the total attenuation coefficient. In XCOM, users can input the characteristics of a material, such as its composition and density, and obtain detailed information on the material's interaction with photons. The software provides data on cross sections for different processes, allowing users to calculate the total attenuation coefficient for a given material at specific photon energies. This information is crucial for designing effective radiation shielding, as it helps assess how materials absorb and scatter radiation, guiding the selection of optimal shielding materials for various applications, including medical, industrial, and research settings. The XCOM software, through its photon cross-section database, aids in understanding and quantifying the attenuation of radiation, providing valuable insights for radiation protection and shielding design.

4. Results and Discussion

The figures presented, Figure 1 and Figure 2, have been generated using the XCOM software. These figures specifically focus on the attenuation properties of metal hydrides, which are predominantly utilized in the storage of hydrogen in solid form. The objective of these figures is to illustrate the effects of high-energy radiation on the study of various metal hydrides. Figure 1, depicts the impact of high-energy radiation on different metal hydrides without considering coherence scattering. The attenuation values for each metal hydride are showcased, providing insights into how these materials interact with radiation. The data presented in Figure 1 allows for a comprehensive understanding of the attenuation characteristics of metal hydrides in the absence of coherence scattering. Figure 2 explores the same set of metal hydrides but takes into account coherence scattering. Coherence scattering refers to the phenomenon where the phase relationships of the scattered waves are maintained. Including this aspect in the analysis provides a more nuanced perspective on how these metal hydrides respond to high-energy radiation. Figure 2 thus presents the attenuation data with coherence scattering considered, offering a more comprehensive view of the interaction between metal hydrides and radiation.

The significance of these figures lies in their contribution to the understanding of the behavior of metal hydrides under highenergy radiation conditions. This information is particularly relevant given the prevalent use of metal hydrides in solid-state hydrogen storage applications. Researchers and professionals in fields related to materials science, hydrogen storage, and radiation studies can benefit from the insights provided by these figures, aiding in the development and optimization of materials for practical applications in hydrogen storage systems.

4.1 Total attenuation without Coherence scattering

The investigation into the nature of the TAC without SC is detailed in Figure 1. The analysis encompasses various metal hydrides commonly employed in solid-state hydrogen storage applications. The findings reveal distinctive trends in TAC across the considered energy spectrum (from 10⁻³ to 10 MeV). In the lower energy region (10⁻³ to 10 MeV), Figure 1 illustrates that the TAC of LiBH₄ is notably lower compared to the other metal hydrides under examination. This could be attributed to the unique composition and molecular structure of LiBH4, influencing its interaction with radiation at lower energy levels. On the contrary, Mg₂NiH₄ exhibits a higher TAC than the other metal hydrides in this range, suggesting a greater propensity to attenuate radiation. However, as the energy level increases, a distinct shift in dominance is observed. In the higher energy region, FeTiH₂ emerges as the dominant metal hydride, showcasing a higher TAC than its counterparts. This implies that FeTiH₂ possesses superior attenuation properties when subjected to higher-energy radiation. Notably, LiBH4 maintains its lower TAC across both lower and higher energy regions, suggesting a consistent behavior in response to varying energy levels. It is imperative to acknowledge that these observations are made under the assumption of non-coherence in the scattering process. In other words, coherence scattering effects, which maintain phase relationships in scattered waves, are not considered in this analysis. This assumption is justified based on the specific conditions and parameters of the study. The contrasting behaviors observed among the metal hydrides underscore the significance of tailoring materials for specific radiation conditions. For instance, while LiBH4 may be preferred in scenarios where lower TAC is desirable, FeTiH₂ could find application in contexts where superior attenuation at higher energy levels is crucial. This nuanced understanding contributes to the broader field of materials science and aids in the strategic selection and design of metal hydrides for optimal performance in hydrogen storage applications under diverse radiation conditions.

Within the energy range spanning from 10⁻¹ to 10 MeV, a noteworthy observation emerges concerning the Total Attenuation Coefficient (TAC) of each metal hydride. In this interval, the TAC values for the different metal hydrides exhibit a remarkable proximity, indicating a comparable behavior across this energy spectrum. This uniformity implies that, within this broad range, the attenuation characteristics of the considered metal hydrides are relatively consistent. A more intricate pattern unfolds in the narrow energy region between 10⁻³ to 10⁻² MeV. Within this specific range, the TAC experiences a pronounced and abrupt decrease, followed by a sharp increase for each of the considered metal hydrides. This distinctive trend suggests a unique energy response within this narrow interval. The initial decrease may be attributed to certain energy-absorbing mechanisms or resonance phenomena specific to the molecular structures of the metal hydrides under scrutiny. Subsequently, the sharp increase could signify the onset of different interaction mechanisms that lead to enhanced attenuation.

Beyond this specific energy region, the TAC behaviors of the remaining metal hydrides appear to be more analogous, exhibiting a shared nature. However, it is noteworthy that two metal hydrides, FeTiH₂ and Mg₂NiH₂, deviate from this general trend. In these instances, the TAC profiles showcase two distinct deep points and peak points, setting them apart from the rest of the metal hydrides, which typically exhibit a single peak at the initial phase. The presence of two deep points and peak points in FeTiH₂ and Mg₂NiH₂ suggests a more complex response to radiation within this energy range. These specific metal hydrides may possess unique molecular structures or composition characteristics that result in multiple attenuation mechanisms or resonances occurring at different energy levels. Such intricacies in the TAC profiles of FeTiH₂ and Mg₂NiH₂ underline the importance of considering the nuanced nature of different metal hydrides when assessing their suitability for various applications, especially in contexts where specific energy ranges are of significance.

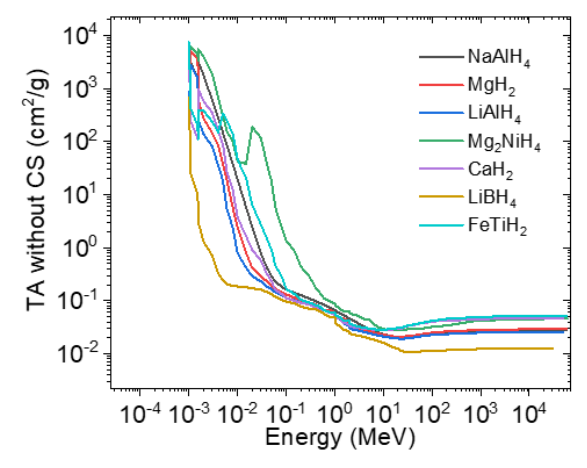


Figure 1: Total attenuation without coherence scattering with energy

4.2 Total attenuation with Coherence scattering

The TAC with coherence scattering exhibits a general similarity to the TAC without coherence scattering, reflecting comparable trends in most of the energy range. However, notable distinctions become evident when examining specific energy regions. In the lower energy region, below 1 MeV, the TAC with coherence scattering deviates from its non-coherence counterpart. Here, we observe a significant difference, indicating that the inclusion of coherence scattering has a discernible impact on the attenuation behavior of the material. The lower TAC in this energy range with coherence scattering suggests that the coherent nature of scattering processes influences the overall attenuation, potentially leading to enhanced absorption or altered scattering patterns. Contrastingly, in the higher energy region, the TAC profiles with and without coherence scattering tend to converge, demonstrating a higher degree of similarity. In this energy range, coherence scattering seems to have a less pronounced effect on the overall attenuation characteristics. The convergence implies that at higher energies, other factors or mechanisms dominate the attenuation process, overshadowing the influence of coherence scattering.

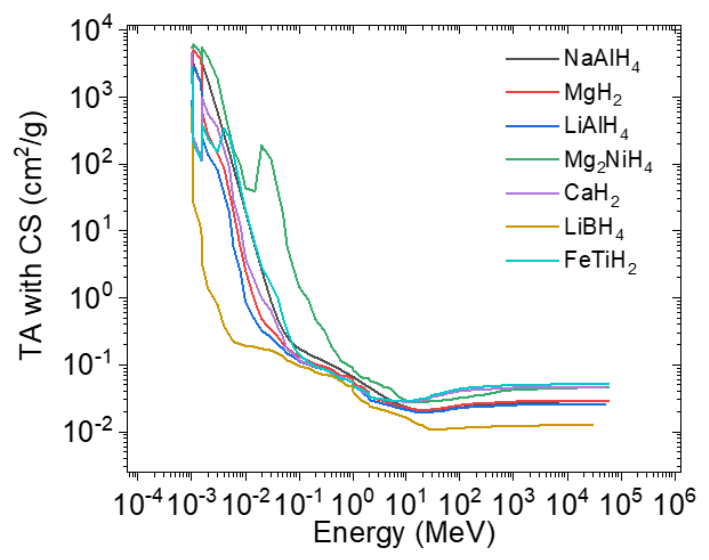


Figure 2: Total attenuation with coherence scattering with energy

The observed differences in the lower energy region may be attributed to the specific interactions between the incident radiation and the material's atomic or molecular structure. Coherence scattering, involving maintained phase relationships in the scattered waves, may play a more significant role in this energy range, altering the overall attenuation response. Understanding these distinctions becomes crucial for applications where control over radiation attenuation, especially in specific energy ranges, is imperative. The nuanced influence of coherence scattering in the lower energy region may open avenues for tailored material design or optimization to achieve desired attenuation characteristics.

5. Conclusion

In conclusion, the study of TAC with and without coherence scattering reveals nuanced behavior in response to varying energy levels. The inclusion of coherence scattering influences TAC, particularly in the lower energy region (below 1 MeV), where a notable decrease is observed. This suggests that coherent scattering processes play a significant role in shaping attenuation characteristics, affecting absorption and scattering patterns. However, in the higher energy region, coherence scattering has a diminished impact, and TAC profiles with and without coherence scattering become more similar. These findings underscore the importance of considering coherence scattering effects, especially in applications requiring precise control over radiation attenuation. The observed distinctions provide valuable insights for material design and optimization, allowing for tailored attenuation properties in diverse energy scenarios.

REFERENCES

- [1] Zaluska, A., Zaluski, L., Ström-Olsen, J. O. (2000). Sodium alanates for reversible hydrogen storage. Journal of Alloys and Compounds, 298(1-2), 125-134. DOI: 10.1016/S0925-8388(99)00666-0
- [2] Suttisawat, Y., Rangsunvigit, P., Kitiyanan, B., Kulprathipanja, S. (2010). A reality check on using NaAlH4 as hydrogen storage material. Journal of Solid State Electrochemistry, 14(10), 1813-1819. DOI: 10.1007/s10008-010-1019-7
- [3] Mekky, A. H. (2023). Electronic structure and stability of pure sodium alanate clusters Na12Al12H48, and the interstitial space-doped with Ti, C and H atoms, as a promising hydrogen storage system: Density functional theory. International Journal of Hydrogen Energy, 48(53), 20430-20440.
- [4] Song, M., Zhang, L., Wu, F., Zhang, H., Zhao, H., Chen, L., Li, H. (2023). Recent advances of magnesium hydride as an energy storage material. Journal of Materials Science & Technology, 149. 99-111.
- [5] Hou, Q., Yang, X., Zhang, J. (2021). Review on Hydrogen Storage Performance of MgH2: Development and Trends. ChemistrySelect, 6(7), 1589-1606. DOI: 10.1002/slct.202004476
- [6] Fruchart, D., Jehan, M., Skryabina, N., de Rango, P. (2023). Hydrogen Solid State Storage on MgH2 Compacts for Mass Applications. Metals, 13, 992. DOI: 10.3390/met13050992
- [7] Liu, Z., Liu, J., Wei, S., Xia, Y., Cheng, R., Sun, L., ... Zhang, G. (2023). Improved hydrogen storage properties and mechanisms of LiAlH4 doped with Ni/C nanoparticles anchored on large-size Ti3C2Tx. Journal of Alloys and Compounds, 931, 167353.
- [8] Pratthana, C., Yang, Y., Rawal, A., Aguey-Zinsou, K. F. (2022). Nanoconfinement of lithium alanate for hydrogen storage. Journal of Alloys and Compounds, 926, 166834.
- [9] Baraban, A. P., Chernov, I. A., Dmitriev, V. A., Elets, D. I., Gabis, I. E., Kuznetsov, V. G., ... Voyt, A. P. (2022). The Mg2NiH4 film on nickel substrate: synthesis, properties and kinetics of formation. Thin Solid Films, 762, 139556.

- [10] Baraban, A. P., Dmitriev, V. A., Gabis, I. E., Voyt, A. P., Klyamkin, S. N., Shikin, I. V. (2023). Direct synthesis of Mg2NiH4 from MgH2 and Ni. Physics of Complex Systems, 4(3), 94-102. DOI: 10.33910/2687-153X-2023-4-3-94-102
- [11] Lu, X., Zhang, L., Zheng, J., Yu, X. (2022). Construction of carbon covered Mg2NiH4 nanocrystalline for hydrogen storage. Journal of Alloys and Compounds, 905, 164169.
- [12] Kong, V. C. Y., Kirk, D. W., Foulkes, F. R., Hinatsu, J. T. (2003). Development of hydrogen storage for fuel cell generators II: utilization of calcium hydride and lithium hydride. International Journal of Hydrogen Energy, 28(2), 205-214.
- [13] Nagashima, K., Visbal, H., Hirao, K., Kamisawa, A. (2015). Modification of Calcium Hydride as Solid Hydrogen Source for Fuel Cell System. International Journal of Applied Ceramic Technology, 13(2). DOI: 10.1111/ijac.12508
- [14] Balakrishnan, S., Humphries, T. D., Paskevicius, M., Buckley, C. E. (2023). Thermodynamic and kinetic properties of calcium hydride. International Journal of Hydrogen Energy, 48(78), 30479-30488.
- [15] Assila, A., Rkhis, M., Sebbahi, S., Hajjaji, A. (2024). Improvement of the thermodynamic properties of lithium borohydride LiBH4 by mechanical treatment for hydrogen storage applications: A DFT investigation. International Journal of Hydrogen Energy, 51. 72-78. DOI: 10.1016/j.ijhydene.2023.10.317
- [16] Züttel, A., Wenger, P., Rentsch, S., Emmenegger, Ch. (2003). LiBH4 a new hydrogen storage material. Journal of Power Sources, 5194(1), 1-7. DOI: 10.1016/S0378-7753(03)00054-5
- [17] Zhang, Y. H., Li, C., Yuan, Z., Zhao, D. (2022). Research progress of TiFe-based hydrogen storage alloys. Journal of Iron and Steel Research International, 29(4). DOI: 10.1007/s42243-022-00756-w
- [18] Dragassi, M.-C., Royon, L., Redolfi, M., Ammar, S. (2023). Hydrogen Storage as a Key Energy Vector for Car Transportation: A Tutorial Review. Hydrogen, 4, 831-861. DOI: 10.3390/hydrogen4040051
- [19] Ramírez-Malo, J. B., Márquez, E., Villares, P., & Jiménez-Garay, R. (1992). Determination of the Refractive Index and Optical Absorption Coefficient of Vapor-Deposited Amorphous As-S Films Transmittance Measurements. Journal 133(2), 499-507. from Name, https://doi.org/10.1002/pssa.2211330234